Kivirikko, K. I., and Prockop, D. J. (1967a), *Arch. Biochem. Biophys. 118,* 611.
Kivirikko, K. I., and Prockop, D. J. (1967b), *J. Biol. Chem. 242,* 4007.
Kivirikko, K. I., Suga, K., Kishida, Y., Sakakibara, S., and Prockop, D. J. (1971), *Biochem. Biophys. Res. Commun. 45,* 1591.
McClure, W. R., and Jovin, T. M. (1975), *J. Biol. Chem. 250,* 4073.
McGee, J. O'D., Rhoads, R., and Udenfriend, S. (1971), *Arch. Biochem. Biophys. 144,* 343.
Olsen, B. R., Hoffmann, H.-P., and Prockop, D. J. (1976), *Arch. Biochem. Biophys. 175,* 341.
Prockop, D. J., Berg, R. A., Kivirikko, K. I., and Uitto, J. (1976), in Biochemistry of Collagen, Ramachandran, G. N., and Reddi, A. H., Ed., New York, N.Y., Plenum Press, p 163.
Rosenbloom, J., Harsch, M., and Jimenez, S. (1973), *Arch. Biochem. Biophys. 158,* 478.
Rupley, J. A. (1967), *Proc. R. Soc. London Ser. B, 167,* 416.
Sakakibara, S., Kishida, Y., Kikuchi, Y., Sakai, R., and Kakiuchi, K. (1968), *Bull. Chem. Soc. Jpn. 41,* 1273.
Sakakibara, S., Shimonishi, Y., Kishida, Y., Okada, M., and Sugihara, H. (1967), *Bull. Chem. Soc. Jpn. 40,* 2164.
Sherman, L. A., and Gefter, M. L. (1976), *J. Mol. Biol. 103,* 61.
Sutoh, K., and Noda, H. (1974a), *Biopolymers 13,* 2477.
Sutoh, K., and Noda, H. (1974b), *Biopolymers 13,* 2461.
Tanzer, M. L., Church, R. L., Yaeger, J. A., Wampler, D. E., and Park, E.-D. (1974), *Proc. Natl. Acad. Sci. U.S.A. 71,* 3009.
Traub, W., and Piez, K. A. (1971), *Adv. Protein Chem. 25,* 243.
Tuderman, L., Kuutti, E.-R., and Kivirikko, K. I. (1975), *Eur. J. Biochem. 52,* 9.

A Confirmation of the Phase Behavior of *Escherichia coli* Cytoplasmic Membrane Lipids by X-Ray Diffraction†

Carol D. Linden,‡ J. Kent Blasie,* and C. Fred Fox*

ABSTRACT: The lipid fatty acid composition of the cytoplasmic membranes of *Escherichia coli* can be varied by growing an unsaturated fatty acid auxotroph in the presence of different fatty acid supplements. Electron spin resonance (ESR) studies of spin-label partitioning into the cytoplasmic membranes of different lipid fatty acid compositions as a function of temperature have been interpreted as indicating a broad order-to-disorder transition in the membrane lipids, the end points of the transition depending upon the fatty acid composition. We have utilized x-ray diffraction to confirm the ESR studies for three different fatty acid supplements (oleic, elaidic, and bromostearic). We found that the characteristic end-point temperatures detected by ESR were indeed the end-point temperatures of a broad order-to-disorder transition of the cytoplasmic membrane lipids. In addition, Patterson functions calculated from lamellar x-ray diffraction from partially oriented cytoplasmic membranes indicate a decrease in average membrane thickness upon fatty acid chain melting.

Upon melting or freezing, lipids in intact membranes or in extracted form undergo a broad phase transition (Luzzati, 1968; Engleman, 1970). This broad transition is defined by distinct end points and can be described using phase diagrams. Electron spin resonance (ESR)[1] has been used to define the end points of the phase transition in binary lipid mixtures (Shimshick and McConnell, 1973). A lower characteristic temperature (t_l) marks the onset of melting. Melting of the two components continues as temperature is increased until an upper characteristic temperature (t_h) is reached. Below t_l all lipid is in a frozen state; above t_h, all lipid is in a liquid state. Hence, t_l lies on the solidus curve and t_h lies on the fluidus curve of the phase diagram for the system. Over the temperature range bounded by t_l and t_h, there exists an equilibrium mixture of fluid and solid lipid phases; this equilibration requires lateral diffusion (Kornberg and McConnell, 1971; McConnell et al., 1972).

The spin-label probe Tempo was used in ESR studies of cytoplasmic membranes isolated from cells of an unsaturated fatty acid auxotroph of *E. coli* grown with single fatty acid supplements (Linden et al., 1973b). Partitioning of Tempo between hydrocarbon and aqueous phases of the membranes revealed that there were two characteristic temperatures defining the course of melting of the membrane lipids. Aqueous dispersions of lipids extracted from these membranes were examined in the same manner and yielded similar characteristic temperatures. By analogy with ESR studies of model binary lipid mixtures, these temperatures were designated as the upper and lower characteristic temperatures of the membrane lipid phase transition. This analogy is appropriate since analysis of the membrane phospholipid fatty acid composition and

† From the Molecular Biology Institute and the Department of Bacteriology, University of California, Los Angeles, California 90024 (C.F.F.), and the Department of Biochemistry and Biophysics, University of Pennsylvania, Philadelphia, Pennsylvania 19174 (J.K.B.). *Received March 4, 1975.* Supported in part by United States Public Health Service Research Grants GM-18233 and GM-12202.
‡ Predoctoral trainee supported by United States Public Health Service Grant GM-1531. Current address: Division of Chemistry, California Institute of Technology, Pasadena, California 91109.
* Recipients of United States Public Health Service Research Career Development Awards from the National Institute of General Medical Sciences.
[1] Abbreviations used: Tempo, 2,2,6,6-tetramethylpiperidinyl-1-oxyl; ESR, electron spin resonance.

distribution revealed that the membrane lipids of cells grown with certain fatty acid supplements closely approximate a binary lipid system (Linden et al., 1973a).

β-Glucoside and β-galactoside transport, which are mediated by two independent membrane localized systems, were examined in unsaturated fatty acid auxotrophs grown with a number of single fatty acid supplements (Linden et al., 1973b; Linden and Fox, 1973). Arrhenius plots of the log of the rate of transport vs. the reciprocal of absolute temperature revealed two slope intercepts which correlated with the characteristic temperatures defined by the ESR studies (Linden et al., 1973b).

Although there was no real doubt from these and earlier observations (Wilson et al., 1970; Wilson and Fox, 1971; Overath et al., 1970) that the boundaries of the phase transition can be defined by spin-label partitioning and that events occurring at these boundaries affect membrane functions such as sugar transport, we felt it desirable to obtain confirmatory evidence using a more direct technique.

Engelman was the first to use x-ray diffraction to demonstrate that frozen and liquid domains of lipid fatty acid chains could be detected relative to the broad thermal phase transition in membranes (Engelman, 1970, 1971). As in the case of synthetic lipid systems, domains of frozen fatty acid chains gave rise to sharp high-angle diffraction at an equivalent Bragg spacing of 4.2 Å and domains of melted chains to diffuse diffraction at 4.6 Å (Luzzati, 1968; Levine and Wilkins, 1971; Wilkins et al., 1971). Similarly, Esfahani et al. (1971) detected frozen and liquid domains of lipid fatty acid chains in membranes isolated from *E. coli*. Dupont et al. (1972) employed novel instrumentation to detect the kinetics of formation of such liquid and frozen domains in bacterial membranes. The utility of x-ray diffraction for detecting the characteristic end points of broad order-to-disorder lipid transitions in membranes, t_l and t_h, has recently been critically reviewed (Engelman, 1975).

Since x-ray diffraction provides a means of directly assessing the physical state of membrane lipid domains as well as the possibility of determining the effect of their physical state on the average profile structure of the membrane (Engelman, 1971), we undertook an x-ray diffraction study of cytoplasmic membranes isolated from an unsaturated fatty acid auxotroph of *E. coli* grown in medium supplemented with oleic, elaidic, or bromostearic acids. The purpose of this study was only to confirm that the characteristic end-point temperatures detected by ESR studies of spin-label partitioning were indeed the end-point temperatures of a broad order-to-disorder transition of the cytoplasmic membrane lipids and that the physical state of the membrane lipid domains affected the average profile structure of the membrane in the usual manner. In no way was this x-ray diffraction study intended to represent a thorough investigation of the entire phase diagram of the *E. coli* cytoplasmic membrane lipids or a thorough analysis of the structure of this membrane. This study represents the first instance in which data obtained from ESR, x-ray diffraction, and physiological studies with a single organism have been correlated.

Materials and Methods

1. Growth and Properties of Bacteria. Strain 30Eβox$^-$ was used exclusively in the studies reported here. It is an unsaturated fatty acid auxotroph of *E. coli* strain K12, defective in the β oxidation of fatty acids. The properties of the parent strain (Wilson et al., 1970; Wilson and Fox, 1971) and of this mutant (Linden et al., 1973b) have been described. Cells were cultured in medium A (Davis and Mingioli, 1950) supplemented with 1% Difco casamino acids, 5 μg/mL of thiamine-HCl, 0.5% of the nonionic detergent Triton X-100 (Rohm and Haas), and 0.02% of an essential fatty acid. Elaidic (*trans*-9-octadecenoic) and oleic (*cis*-9-octadecenoic) acids were purchased from the Hormel Institute, Austin, Minn. Bromostearic acid (a mixture of 9- and 10-bromostearic acids) was prepared by a published procedure (Fox et al., 1970; Jungermann and Spoerri, 1958). Cultures of 500 mL were grown with vigorous rotary agitation at 37 °C in 2-L flasks. Cultures provided with a bromostearate supplement were grown at 40 °C. Cells were grown with the indicated essential fatty acid for at least three doublings of cell mass. Growth was followed turbidimetrically at 420 nm.

2. Preparation of Membranes. Isolation of inner (cytoplasmic) membranes has been described in detail (Fox et al., 1970). Membrane preparations were stored at −70 °C prior to use. This procedure (freezing and thawing) yields flat sheets of membrane fragments rather than vesicles as observed by transmission electron microscopy (Li and Fox, 1975); this facilitates the partial orientation of membrane fragments upon sedimentation. Membranes were pelleted for preparation of concentrated dispersions for x-ray studies by centrifuging at 20 000 rpm for 45 min to 1 h in a Spinco SW27 rotor. The pellet was dispersed by gentle swirling with a spatula and introduced into a small volume chamber sealed with Mylar windows. Partially oriented membrane pellets were prepared by sedimenting approximately 5 mg as membrane protein onto a thin foil strip. Centrifugation was for 2 h at 25 000 rpm in an SW27 rotor. The resultant pellets were approximately 0.5-mm thick. The foil strips were mounted on curved glass holders and equilibrated at 90% relative humidity at 0–4 °C for at least 4 h.

3. X-Ray Diffraction. High-angle diffraction patterns from oriented pellets at grazing incidence or dispersions were obtained with approximately 4-h exposures using an Elliott toroid point-focus camera powered by a Jarrell-Ash x-ray generator. Low-angle diffraction patterns were obtained from oriented membrane pellets at grazing incidence with 10-h exposures using a modified Franks camera powered by an Elliott rotating-anode x-ray generator; a line focus of 0.35 × 0.5 mm at the guard slits was used with the beam height parallel to the specimen surface. The x-ray beam in both cameras was nickel-filtered Cu Kα radiation through a vacuum path. Sample temperature was controlled by circulating water from a temperature controlled Neslab water bath through the aluminum sample holder. The water content of the oriented pellets was maintained with a stream of moist helium at a defined relative humidity of 90–95%. Ilford Industrial G x-ray film was used to record diffraction patterns. The films were traced using a Joyce Loebl Mark III CS microdensitometer; tracings were corrected for the known camera background and water diffraction.

Results

(*a*) *High-Angle Diffraction.* The corrected microdensitometer tracings of the diffraction arising from dispersions of elaidate membranes at temperatures above, below, and within the phase transition are shown in Figure 1. The specimen to film distance, in this case ~50 mm, could be measured relatively accurately since it was possible to determine the center of the specimen holder for dispersions. It was also possible to determine the center of the film and, thus, calculate the Bragg spacings of the diffraction maxima. At 25 °C, a sharp diffraction ring at 4.2 ± 0.1 Å was observed. By comparison with

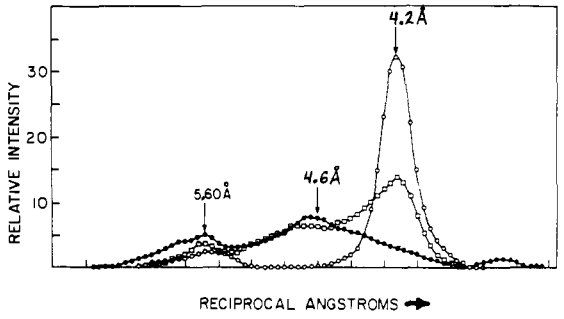

FIGURE 1: Corrected microdensitometer tracings of the high-angle diffraction arising from a dispersion of cytoplasmic membranes of cells grown with an elaidic acid supplement. Intensity is defined in arbitrary units. X-ray films of the diffraction patterns were obtained and characterized as described in the text. (○) Sample held at 25 °C. (□) Sample held at 36 °C. (●) Sample held at 42 °C.

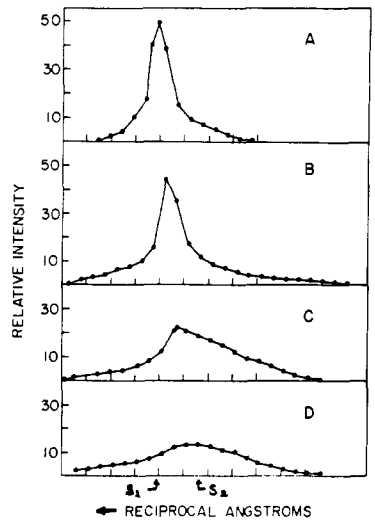

FIGURE 2: Corrected microdensitometer tracings of the high-angle diffraction at approximately right angles to the lamellar diffraction arising from partially oriented pellets of cytoplasmic membranes of cells grown with an oleic acid supplement. Intensity is defined in arbitrary units. X-ray films of the diffraction patterns were obtained and characterized as described in the text. (A) Sample held at 9–10 °C. (B) Sample held at 15–16 °C. (C) Sample held at 25 °C. (D) Sample held at 28–30 °C.

x-ray diffraction data obtained from other systems (Engelman, 1970, 1971), it was possible to assign the sharp diffraction at this position to domains of lipid hydrocarbon chains in the crystalline state. This result is in excellent agreement with ESR data obtained with these membranes (Linden et al., 1973b). At 42 °C, a broad, diffuse diffraction band was observed, its maximum occurring at 4.6 ± 0.1 Å. This diffraction arises from domains of lipid hydrocarbon chains in the melted, or liquid-crystalline state, and corresponds to the temperature at which melted chains are observed in the same membranes using ESR. At 36 °C, a sharp diffraction ring was observed at ~4.2 Å which broadened on the low-angle side to merge with a less intense, broader diffraction band at ~4.6 Å. This pattern indicates the simultaneous presence of frozen and melted domains of lipid hydrocarbon chains and is also in agreement with the data obtained by ESR. The constant diffraction maximum at 5.6 Å arises from the windows on the specimen chamber.

Entirely similar results were obtained with partially oriented pellets of elaidate membranes at 90–95% relative humidity. Below 30 °C, only diffraction arising from frozen hydrocarbon chain domains could be detected. From above 30 to 38 °C, both frozen and melted chain domains were detected, and, above 38 °C, only melted chain domains were observed. An experiment was performed where patterns were obtained from the same sample at 38, 39, and then 38 °C. The diffraction patterns at 38 °C before and after raising the sample to 39 °C were identical; both frozen and melted chain domains were observed. At 39 °C, only melted chain domains were observed.

Figure 2 shows the corrected microdensitometer tracings of diffraction patterns obtained with the toroid camera from partially oriented pellets of membranes from cells grown with an oleate supplement. The specimen-to-film distance (~50 mm) could only be estimated for the oriented pellets mounted at grazing incidence since it was not possible to determine the exact center of the pellet's scattering volume at grazing incidence when mounted on its curved glass holder. Hence, we shall describe the results from this and subsequent speciments in a somewhat more qualitative manner. Figures 2A, B, C, and D show the high-angle diffraction arising from the membrane pellet at 9–10, 15–16, 25, and 28–30 °C, respectively. At 9–10 °C, the sharp diffraction maximum at the position denoted by s_1 (s_1 generally occurs at 4.2 ± 0.2 Å) in the figure indicates the presence of predominately crystalline hydrocarbon chain domains. At 15–16 °C, this predominate sharp maximum shifted slightly toward low angles and showed a slight broadening on the low-angle side. At 25 °C, the diffraction broadened considerably due primarily to a much larger broad component with a maximum in the region of s_2 (s_2 generally occurs at 4.6 ± 0.2 Å). The considerable broadening of this peak only at lower angle indicates the presence of melted hydrocarbon chain domains, while the sharp high-angle side of the peak suggests that some crystalline hydrocarbon chain domains were still present in the sample at this temperature. At 28–30 °C, only a broad diffraction maximum appeared in the region of s_2 and the sharp shoulder on its high-angle side disappeared. At this temperature the hydrocarbon chain domains were completely melted.

Microdensitometer tracings of the high-angle diffraction arising from pellets of partially oriented bromostearate membranes obtained with the modified Franks camera showed (using the terminology described above) a sharp reflection at s_1 at 9–10 °C, a sharp reflection at s_1 plus a broad diffraction band at s_2 at 19–20 °C and only a broad diffraction band at s_2 at temperatures at and above 24 °C. Thus, at 9–10 °C, essentially all of the membrane phospholipid hydrocarbon chain domains were in a crystalline state, at 19–20 °C both crystalline and melted chain domains were present and above 24 °C the chain domains were all in the melted state.

The comparisons between characteristic temperatures for membranes of cells grown with the three fatty acid supplements determined by ESR and x-ray techniques are summarized in Table I.

(*b*) *Low-Angle Diffraction.* Lamellar diffraction patterns in the low-angle region were obtained with partially oriented pellets of oleate membranes using grazing incidence with the modified Franks camera. From the observed lamellar diffraction, it was possible to calculate the membrane thickness at various temperatures. A computer-calculated Patterson function was used to obtain these data from the digitized corrected lamellar intensities. The Patterson function is the Fourier transform of the corrected continuous lamellar intensity data. Corrections for loss of intensity due to sample absorption, the type of beam focus (line), and specimen geometry were incorporated into the calculations (Lesslauer et al., 1972). The interpretation of these types of low-resolution

TABLE I: Comparison of Characteristic Temperatures of the Lipid-Phase Transition as Determined by X-Ray Diffraction and the Partitioning of Spin Labels.

Fatty Acid Supplement	t_l		t_h	
	ESR[a]	X-Ray[b]	ESR[a]	X-Ray[b]
Elaidate	30.7	30–32	37.7	38–39
Oleate	15.8	15–16	31	28–30
Bromostearate	<17	>10, <19	22.2	>20, <24

[a] The spin resonance data for elaidate and oleate membranes are from Linden et al. (1973b), and those for bromostearate membranes are from Linden and Fox (1973). The ESR studies with bromostearate membranes were not extended below 17 °C. [b] The accuracy of the determination of the t_l and t_h by x-ray diffraction has recently been critically reviewed by Engelman (1975). The accuracy of determining t_l normally depends on the relatively more difficult measurement of the *disappearance* of *broad diffuse diffraction* arising from the few remaining domains of melted lipid fatty acid chains. Hence, even though the integrated area of the sharp diffraction arising from the domains of frozen fatty acid chains may not increase significantly for temperatures several degrees below the t_l values reported here, we certainly cannot prove that there are no melted chain domains existing in the membranes below these t_l values.

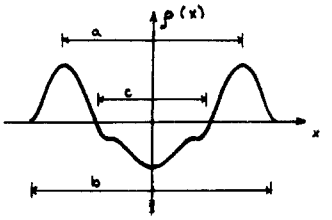

FIGURE 3.

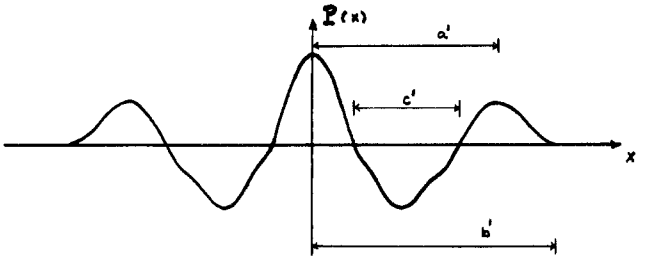

FIGURE 4.

functions is based on the typical phospholipid bilayer membrane electron density profile (Levine and Wilkins, 1971) shown in Figure 3. In this profile, the two outer peaks above the baseline electron density of water represent the polar head groups of phospholipids arranged in a bilayer configuration. The broad central trough of electron density less than that of water represents the low electron density hydrocarbon region in the interior of the bilayer. The arrows marked *a*, *b*, and *c* show the average head-group-to-head-group distance and the resolution-limited total membrane and hydrocarbon core thicknesses, respectively. The autocorrelation function of this type of profile, which need not necessarily be symmetric about $x = 0$, is generally as shown in Figure 4, where c' gives the approximate resolution-limited hydrocarbon core thickness and either a' or b' can be used as measures of the approximate membrane thickness. For an oriented multilayer of membrane fragments which is perfectly ordered (stacked) with periodicity d, this autocorrelation function of the membrane electron density profile occurs in the Patterson function $P(x)$ identically about $x = 0, \pm d, \pm 2d, \ldots$. If simple lattice disorder occurs within the multilayer, this autocorrelation function occurs unperturbed about $x = 0$ in $P(x)$, but occurs about $\pm d, \pm 2d, \ldots$ with progressively decreased amplitude and increased broadening or smearing due to the lattice disorder (Schwartz et al., 1975). In the case of excessive lattice disorder, $P(x)$ contains only the unperturbed autocorrelation function of the membrane profile about $x = 0$. The partially oriented pellets (multilayers) of the *E. coli* cytoplasmic membrane fragments very nearly evidence this extreme degree of lattice disorder in their Patterson functions, since $P(x > a') \ll P(x = 0)$ in the cases studied. As a result of this rather large degree lattice disorder in the *E. coli* membrane multilayers, each membrane fragment, although oriented relative to the sedimentation axis, scatters rather independently of the other membrane fragments without any major interference of such scattering from neighboring fragments in the multilayers. An electron density profile of a sample can be obtained only if reasonably accurate phase assignments for the lamellar intensity maxima can be determined. Since the samples used in this study were partially oriented highly disordered multilayers of membrane fragments with possibly asymmetric electron density profiles, it was impossible to estimate phase assignments and thus only the Patterson function, which can be determined directly from experimental data, was calculated. Figure 5 shows the Patterson functions obtained from oleate membranes at 33 °C (A) and 10 °C (B). These temperatures were chosen so that data could be obtained on totally "liquid" and totally "frozen" membranes with regard to the lipid hydrocarbon chain domains. From Figures 5A and 5B it was calculated that oleate supplemented membranes in the "liquid" state have an average thickness a' of approximately 55 Å and similarly in the "frozen" state of approximately 65 Å. These data correspond well with the data from model membrane and other natural membrane systems which show that, when the membrane lipid hydrocarbon chain domains are in a crystalline state, the membrane is thicker than when the hydrocarbon chain domains are in a melted or liquid-crystalline state (Engelman, 1970, 1971; Cain et al., 1972).

Discussion

Linden et al. (1973b) reported that Arrhenius plots for β-glucoside transport in cells of the *E. coli* unsaturated fatty acid auxotroph used in the present study ordinarily exhibit changes in slope at two characteristic temperatures. These correlated with characteristic temperatures detected by ESR spectroscopy in membranes isolated from cells grown with a number of different essential fatty acid supplements. On the basis of ESR studies with model binary lipid systems, these characteristic temperatures were interpreted to be at points where the bulk membrane lipid phase assumes a totally solid or liquid state. We have confirmed this conclusion by showing that these characteristic temperatures detected by the partitioning of the spin-label Tempo between the hydrocarbon phase of the membrane lipids and the surrounding aqueous medium are indeed the points where the membrane lipids first begin to freeze or become totally frozen as detected independently by x-ray diffraction (see Table I). Although there has been some recent criticism of the use of spin-label partitioning between the hydrocarbon and aqueous membrane phases to determine the boundaries of the lipid phase transition (Lee et al., 1974), the x-ray diffraction studies reported here clearly validate the earlier work by Linden et al. (1973b) on the plasma membranes of a fatty acid auxotroph of *E. coli* grown with three different fatty acid supplements.

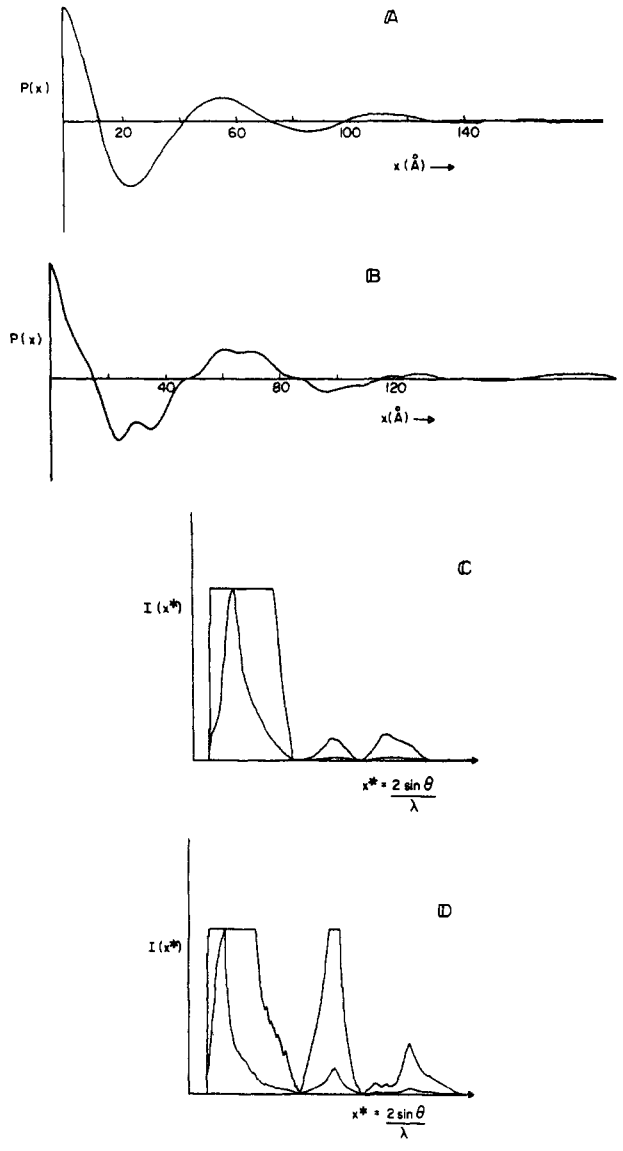

FIGURE 5: Patterson functions calculated from the corrected low-angle lamellar diffraction arising from cytoplasmic membranes of cells grown with oleic acid supplements. (A) Oleate enriched membranes held at 33 °C. (B) Oleate enriched membranes held at 10 °C. X-ray films of the lamellar diffraction patterns were obtained and characterized as described in the text; the corrected lamellar intensity functions obtained from these films are shown (C) at 33 °C and (D) at 10 °C. These intensity functions contain only broad maxima relative to the camera line width all with equivalent mosaic spread. There appears to be no evidence in these diffraction patterns for the formation of separated pure lipid phases in the partially oriented membrane pellets at 90–95% relative humidity.

In addition, we have shown that there are rather dramatic changes occurring in the average thickness of the *E. coli* plasma membrane which depend on the physical state of the membrane lipids. Similar changes in membrane thickness have been observed in membranes from *A. laidlawii* (Engelman, 1970, 1971) and in lipid model membranes (Luzzati, 1968; Cain et al., 1972). This change in thickness occurs because the extension of the frozen lipid hydrocarbon chains is considerably greater than the time-average extension of melted fatty acid chains (Cain et al., 1972). As a result, at temperatures between the upper and lower characteristic temperatures for the membrane lipid phase transition, we would expect those regions within the membrane's mosaic structure containing frozen chains to be substantially thicker than those containing only melted chains. Also, since the composition of the melted regions are continually changing with temperature in this temperature range, the position and extension of integral membrane proteins within the profile structure of these regions may also experience changes relative to the thickness of the membrane hydrocarbon core in such regions.

References

Cain, J., Santillan, G., and Blasie, J. K. (1972), *Membr. Res.*, 3.

Davis, B. D., and Mingioli, E. S. (1950), *J. Bacteriol. 60,* 17.

Dupont, Y., Gabriel, A., Chabre, M., Gulik-Krzywicki, T., and Schechter, E. (1972), *Nature (London), New Biol. 238,* 331.

Engelman, D. M. (1970), *J. Mol. Biol. 47,* 115.

Engelman, D. M. (1971), *J. Mol. Biol. 58,* 153.

Engelman, D. M. (1975), *Biophys. J. 15,* 940.

Esfahani, M., Limbrick, A. R., Knutton, S., Oka, T., and Wakil, S. J. (1971), *Proc. Natl. Acad. Sci. U.S.A. 68,* 3180.

Fox, C. F., Law, J. M., Tsukagoshi, N., and Wilson, G. (1970), *Proc. Natl. Acad. Sci. U.S.A. 67,* 598.

Jungermann, E., and Spoerri, P. E. (1958), *J. Am. Oil Chem. Soc. 35,* 393.

Kornberg, R. D., and McConnell, H. M. (1971), *Proc. Natl. Acad. Sci. U.S.A. 68,* 2564.

Lee, A. G., Birdsall, N. J. M., Metcalfe, J. C., Toon, P. A., and Warren, G. B. (1974), *Biochemistry 13,* 3699.

Lesslauer, W., Cain, J., and Blasie, J. K. (1972), *Proc. Natl. Acad. Sci. U.S.A. 69,* 1499.

Levine, Y. K., and Wilkins, M. H. F. (1971), *Nature (London), New Biol. 230,* 69.

Li, J. K.-K., and Fox, C. F. (1975), *J. Ultrastruct. Res. 52,* 120.

Linden, C. D., and Fox, C. F. (1973), *J. Supramol. Struct. 1,* 535.

Linden, C. D., Keith, A. D., and Fox, C. F. (1973a), *J. Supramol. Struct. 1,* 523.

Linden, C. D., Wright, K. L., McConnell, H. M., and Fox, C. F. (1973b), *Proc. Natl. Acad. Sci. U.S.A. 70,* 2271.

Luzzati, V. (1968), in Biological Membranes, Chapman, D., Ed., London, Academic Press, pp 71–123.

McConnell, H. M., Devaux, P., and Scandella, C. (1972), *Membr. Res.*, 27.

Overath, P., Schairer, H. U., and Stoffel, W. (1970), *Proc. Natl. Acad. Sci. U.S.A. 67,* 606.

Schwartz, S., Cain, J., Dratz, E., and Blasie, J. K. (1975), *Biophys. J. 15,* 1201.

Shimshick, E. J., and McConnell, H. M. (1973), *Biochemistry 12,* 2351.

Wilkins, M. H. F., Blaurock, A. E., and Engelman, D. M. (1971), *Nature (London), New Biol. 230,* 72.

Wilson, G., and Fox, C. F. (1971), *J. Mol. Biol. 55,* 49.

Wilson, G., Rose, S., and Fox, C. F. (1970), *Biochem. Biophys. Res. Commun. 38,* 617.